

Nonlinear Control of Wind Turbines: An Approach Based on Switched Linear Systems and Feedback Linearization

Ralph Burkart, Kostas Margellos and John Lygeros

Abstract—The main contribution of this paper is the development of a nonlinear control technique for the control of individual wind turbines in a wind farm. For this purpose, a control scheme based on feedback linearization and gain scheduled linear quadratic regulator (LQR) is applied to a horizontal axis, variable speed, pitch regulated wind turbine. As a result of the physical constraints of their components, wind turbines operate at different control modes with different control objectives. To capture this hybrid nature, a flexible modeling framework based on the notion of hybrid systems is introduced, and the developed controller is designed so as to operate in all modes and over a wide range of wind speeds. The performance and the efficiency of the proposed approach is validated via simulations, and is compared with standard LQR approaches.

I. INTRODUCTION

The high penetration of wind energy sources in the power network highlighted the necessity of developing advanced control techniques for the control of individual wind turbines, so as to achieve maximal aerodynamical efficiency. Amongst modern installations variable speed, pitch regulated wind turbines are the predominant type. In most cases [1], [2], wind turbines are represented by three-bladed, horizontal axis turbine models, which can operate at variable speed and drive a synchronous or induction generator. A gearbox is normally used to step up the slow speed of the rotor to higher values at the generator side, and then a power converter is employed to fully or partially decouple the generator from the power network. That way, variable speed operation is possible, and hence higher efficiency and longer lifetime, due to the reduced mechanical stresses, is achieved. Since the control of power electronics is a separate research topic and its time constant is much shorter than the other turbine components, in this paper we will ignore the power electronics control and an ideal performance will be assumed [3], [4].

As a result of the stochastic nature of the wind that each wind turbine is exposed to, and due to the physical constraints of its components, wind turbines operate at different control modes. Following the typical characterization of [1], [2], [3], [5], two regions with different control objectives are distinguished (Fig. 1). Specifically, in Region I, for wind speeds above the cut-in value but too low for rated power generation, the main objective is to maximize the power extracted from the wind. On the other hand, for high wind

speeds (Region II), the power should be stabilized to its rated value, so as to prevent the system from being overstressed and ensure safe operation. The former is often referred to as the power optimization mode, whereas the latter as the power limitation mode. Details regarding these two control modes will be given in Section III. Another control objective is to reduce the fatigue of the turbine components (blades, shaft, turbine tower), due to the mechanical loads. The trade off between this objective and achieving maximum power tracking was investigated in [6], where for Region II robust control techniques were employed. From a different point of view in [7] the level of mechanical stresses in wind turbines due to various network disturbances, was quantified. In this paper we will focus on the maximum power tracking objective for both regions of operation, whereas the limitation of the mechanical fatigue will not be investigated further.

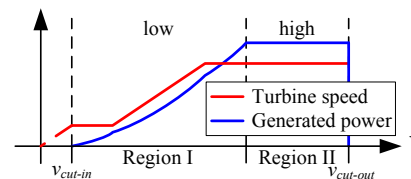


Fig. 1. Wind regions corresponding to different control modes and objectives.

Most of the research on the development of wind turbine controllers is mainly concentrated on linear control techniques, such as standard PID and Linear Quadratic Regulator (LQR) control [2], [8], [9], [10], [11]. These approaches are hampered by the nonlinear behavior that wind turbines exhibit, mainly due to the highly nonlinear dependency of the generated power on the wind. To overcome this drawback, gain scheduling or switching between multiple linear controllers has been proposed. In [4], the authors used a linearized version of the system and applied model predictive control, whereas in [12], [13] training of neural networks and fuzzy logic techniques were used. Even if in some cases the performance of the system is satisfactory, its response to large wind variations may be unpredictable, since these methods are based on linearization and hence are valid only locally. In [14] a multivariable controller using H_2 and H_∞ control techniques was designed. More recent contributions [3], [15] employ nonlinear control based on feedback linearization [16], [17], [18], but are restricted to the power limitation mode of operation. To the best of our knowledge no work has used nonlinear control schemes for

Ralph Burkart, Kostas Margellos and John Lygeros are with the Automatic Control Laboratory, Department of Electrical Engineering, Swiss Federal Institute of Technology (ETH), Physikstrasse 3, ETL 122, 8092, Zürich, Switzerland. email: burkart@ee.ethz.ch, {margellos, lygeros}@control.ee.ethz.ch

the entire operating envelope.

The work of this paper was inspired by [19], where a hierarchical structure for wind turbine control was proposed, consisting mainly of the turbine control and a higher level of supervisory control, which includes the monitoring of the system and determines the appropriate control mode. In this work, we propose a modeling framework based on hybrid automata to capture the interaction between continuous dynamics and discrete transitions forced by the power optimization and power limitation mode of operation. Moreover, a hybrid control scheme, as part of the supervisory control level is designed so as to couple the individual controllers of each region. This paper bridges the formulation and the wind turbine principles of operation described in [2], with the control scheme proposed by [3]. Specifically, for the controller synthesis, the approach of [3], where feedback linearization and LQR were combined, but only for Region II, was extended so as to achieve maximum power tracking, which is the objective of Region I.

The paper is organized as follows. Section II provides details regarding the mathematical modeling, whereas in Section III the control objectives and the resulting hybrid model are presented. Section IV describes in detail the controller synthesis based on feedback linearization and LQR, and Section V illustrates the obtained simulation results. Finally, in Section VI we provide some concluding remarks and directions for future work.

II. MATHEMATICAL MODELING

A. Wind model

Although wind provides the energy that drives the wind turbine, due to its intermittent nature it also acts as a disturbance. Hence the effective wind $v = v_m + v_s$ can be thought of as a superposition of the mean wind speed v_m , which could be either constant or time varying as a result of a sophisticated forecasting method, and a stochastic component v_s . Following [20], [3], the stochastic part v_s can be considered as the point wind after a second order filter, which models the effect of the disc-shaped area swept by the rotor blades. In the frequency domain the power density spectrum S_{v_s} of v_s can be written as $S_{v_s}(f, v_m) = S_p(f)S_f(f, v_m)$, where $S_p(f)$ is the spectrum of the point wind and $S_f(f, v_m)$ denotes the filter, which depends on the mean wind speed. This nonlinear expression can be then approximated by a linear second order transfer function driven by a white noise process.

$$\dot{w}_1 = w_2, \quad (1)$$

$$\dot{w}_2 = -a_1 w_1 - a_2 w_2 + a_3 e, \quad (2)$$

where $w_1 = v_s$, $e \in \mathcal{N}(0, 1)$, and a_1, a_2, a_3 are parameters depending on the mean wind speed.

B. Turbine model

The model of the turbine describes the conversion from wind power to mechanical and in the end electrical power. The power extracted from the wind is given by the nonlinear

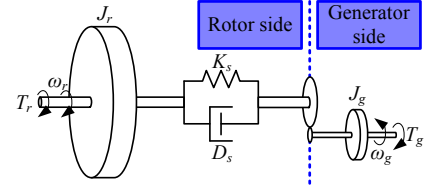


Fig. 2. Schematic diagram of the turbine mechanics.

expression $P_r = \frac{1}{2} \rho \pi R^2 v^3 c_p(\lambda, \theta)$, where ρ is the air density, R is the radius of the blades, and $c_p(\lambda, \theta)$ is the so called efficiency coefficient. The latter depends on the tip speed ratio $\lambda = \frac{\omega_r R}{v}$ and the pitch angle θ . The variable ω_r denotes the speed of the rotor, as shown in the schematic diagram of Fig. 2. Typically, c_p is given by numerical look-up tables. However, in this paper a standard, nonlinear, analytical approximation was used [1], [21].

The conversion from the mechanical energy stored in the rotating blades (speed ω_r , inertia J_r) to electrical power is carried out via a drive train (spring constant K_s , damping coefficient D_s) and a gearbox (gear ratio N_g), which is used to step up the slow speed of the rotor to higher values at the generator side (speed ω_g , inertia J_g). In Fig. 2, T_r and T_g represent the torque at the rotor and generator side respectively. By applying the Newton's laws on that model, one can get the differential equations of ω_r and ω_g (see equation (3)). The dynamics of the twist δ of the flexible drive train are defined by $\dot{\delta} = \omega_r - \frac{\omega_g}{N_g}$. Stress considerations require the differences on the right-hand side of the previous equation to be minimal.

$$\begin{bmatrix} \dot{\omega}_r \\ \dot{\omega}_g \\ \dot{\delta} \\ \dot{\theta} \\ \dot{T}_g \\ \dot{w}_1 \\ \dot{w}_2 \end{bmatrix} = \begin{bmatrix} \frac{P_r(\omega_r, \theta, w_1)}{\omega_r J_r} - \frac{\omega_r D_s}{J_r} + \frac{\omega_g D_s}{J_r N_g} - \frac{\delta K_s}{J_r} \\ \frac{\omega_r D_s}{J_g N_g} - \frac{\omega_g D_s}{J_g N_g^2} + \frac{\delta K_s}{J_g N_g} - \frac{T_g}{J_g} \\ \omega_r - \frac{\omega_g}{N_g} \\ -\frac{1}{\tau_\theta} \theta \\ -\frac{1}{\tau_T} T_g \\ w_2 \\ -a_2 w_2 - a_1 w_1 \end{bmatrix} + \begin{bmatrix} 0 \\ 0 \\ 0 \\ 0 \\ 0 \\ 0 \\ a_3 \end{bmatrix} e. \quad (3)$$

$$+ \begin{bmatrix} 0 & 0 \\ 0 & 0 \\ 0 & 0 \\ \frac{1}{\tau_\theta} & 0 \\ 0 & \frac{1}{\tau_T} \\ 0 & 0 \end{bmatrix} \begin{bmatrix} \theta_r \\ T_{g,r} \end{bmatrix}$$

C. Overall Model

Combining the models for the wind and turbine dynamics, described in the previous subsections, and augmenting the system with first order models for the actuator dynamics (time constants τ_θ, τ_T), leads to the seventh order nonlinear system (3). Let $\dot{x} = f(x) + G_1 u + G_2 e$ denote the above described system, with $x = [\omega_r \ \omega_g \ \delta \ \theta \ T_g \ w_1 \ w_2]^T$. The control input $u = [\theta_r \ T_{g,r}]^T$ comprises of the reference values for the pitch angle and the generator torque. The

numerical values of the model parameters (based on [3]) are given in Table I.

TABLE I
MODEL PARAMETERS.

J_r	90000	[kg·m ²]	$P_{g,nom}$	225	[kW]
J_g	10	[kg·m ²]	$\omega_{r,nom}$	4.29	[rad/s]
K_s	$8 \cdot 10^6$	[Nm/rad]	$\omega_{g,nom}$	105.534	[rad/s]
D_s	$8 \cdot 10^4$	[kg·m ² /(rad·s)]	$\omega_{r,min}$	3.5	[rad/s]
N_g	24.6	[-]	$\omega_{g,min}$	86.1	[rad/s]
R	14.5	[m]	θ_{min}	0	[deg]
τ_θ	0.15	[s]	θ_{max}	25	[deg]
τ_T	0.1	[s]	$ \dot{\theta} _{max}$	10	[deg/s]

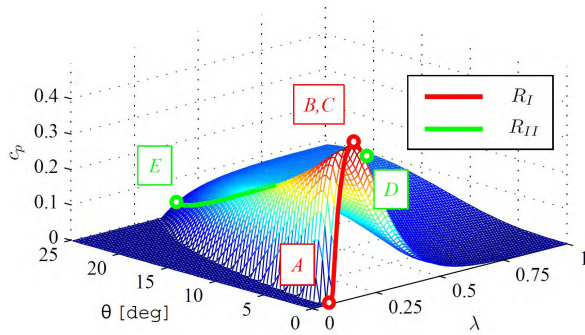


Fig. 3. Power efficiency coefficient $c_p(\lambda, \theta)$ and reference trajectories.

III. WIND TURBINE CHARACTERISTICS AND CONTROL OBJECTIVES

A. Modes of operation and switching conditions

1) **Region I:** Maximum power tracking is the main control objective of Region I. Hence, we aim to maximize the power extracted from the wind. The control inputs θ_r , and $T_{g,r}$ should be properly adjusted so as to maximize c_p . The red curve in Fig. 3 depicts the reference trajectory that the simulated wind turbine should track in Region I. Due to the physical constraints in the generator and rotor speed $[\omega_{g,min}, \omega_{g,nom}] = N_g[\omega_{r,min}, \omega_{r,nom}]$ (see Table I) we distinguish the following parts [2]:

- **A-B:** For wind speeds above v_{cut-in} , λ can be maximized by operating the turbine at $\omega_{r,min}$.
- **B-C:** As soon as c_p reaches its maximum value, ω_r should be adjusted properly to operate the turbine at maximum efficiency.
- **C-D:** In this region, due to high wind speeds, the speed reaches its nominal value $\omega_{r,max}$. Note that although the efficiency decreases the generated power still grows with increasing wind speeds.

As shown in Fig. 3, it is obvious that the pitch angle should be kept at its minimum $\theta_{min} = 0^\circ$ in order to achieve the optimal c_p in Region I. As a consequence, (3) reduces to a single input system in this region. Based on this analysis, the reference trajectories as a function of the mean wind speed v_m , are depicted in Fig. 4.

To define these characteristic curves only the mean wind speed was taken into consideration. However, deviation of

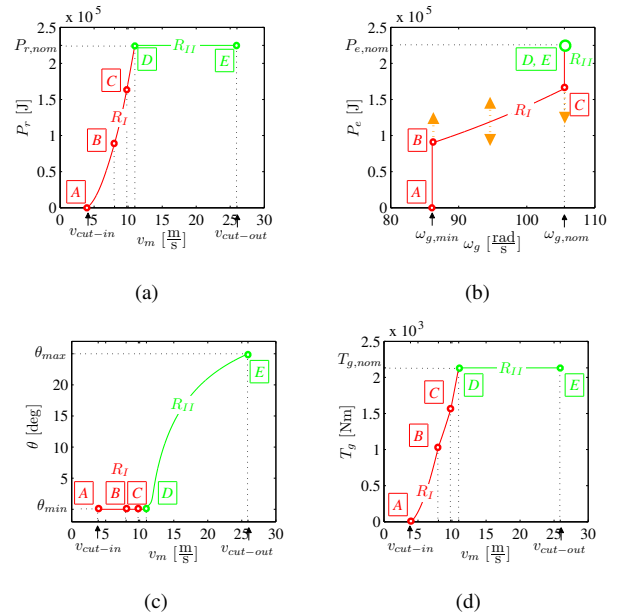


Fig. 4. Reference tracking trajectories: (a) P_r - v_m , (b) P_g - ω_g , (c) θ_r - v_m , (d) $T_{g,r}$ - v_m .

the reference values (indicated by arrows in Fig. 4(b)) is expected due to the stochastic component v_s of the wind. In particular, the turbine dynamics are not fast enough to track changes in the wind speed due to v_s , since the high rotor inertia J_r does not allow immediate adjustments of the tip speed ratio λ . This in turn leads to deviation from the reference trajectory. When the extracted power exceeds the nominal value, the system should switch to the power limitation operating mode.

2) **Region II:** As soon as the generated power $P_g = \omega_g T_g$ reaches its nominal value $P_{g,nom}$ the system must switch mode (Region II), and the new objective is to stabilize P_g , and maintain ω_r at their nominal values. To achieve this, θ is included as an additional control input (see Fig. 3). When the wind speed exceeds its cut-out value $v_{cut-out}$, θ saturates at its maximum $\theta_{max} = 25^\circ$, and in case of higher wind speeds the turbine should be disconnected from the grid. In the case where the pitch angle is fixed to its minimum value (i.e. $\theta = \theta_{min}$), and the power drops from its nominal value (i.e. $P_g < P_{g,nom}$), a transition is enabled and the system switches to the controller of Region I. More details regarding implementation issues so as to achieve smooth transitions and avoid chattering will be given in the next section.

B. Hybrid Model

The switching conditions defined above give rise to discrete transitions, hence the overall model could be represented by the hybrid automaton of Fig. 5. The two modes of operation, denoted by $Q = \{R_I, R_{II}\}$, correspond to the discrete states of the proposed automaton. The continuous evolution is characterized by (3), where following [3], the dynamics are augmented with two additional integrators, so as to avoid steady state error in the power P_g and the rotational speed

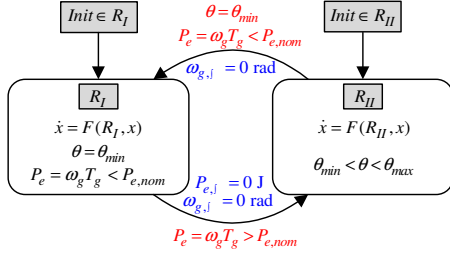


Fig. 5. Hybrid model of the wind turbine system with reset map and guard conditions.

ω_g . Let $P_{g,f}$ and $\omega_{g,f}$ denote the corresponding states. For better switching performance, these states are reseted after each transition. The switching conditions, or in other words the guards, of the hybrid automaton follow from the discussion of the previous section. The corresponding numerical values can be found in Table I. Using the states of the turbine rather than the wind in these conditions, allows for smoother switching and hence undesired overshoots are avoided. Furthermore, this is also an intuitive choice, since accurate measurements of v are rarely provided.

IV. CONTROLLER DESIGN

Inspired by the hybrid model of Fig. 5, two different control strategies were developed. First, a gain scheduled LQR controller was implemented, so as to serve as benchmark for the nonlinear control scheme of Section IV.B, which is the main contribution of the paper. The latter is based on feedback linearization, and LQR is used for the control of the resulting linear system.

A. Gain Scheduled LQR

Infinite horizon LQ control provides an efficient approach for solving unconstrained optimization problems with linear dynamics and quadratic cost functions. For the wind turbine control problem and for each mode of operation $i = 1, 2$, consider the cost $J_i = \int_0^\infty \psi_i(t)^T Q_i \psi_i(t) + v_i(t)^T R_i v_i(t) dt$, that we seek to optimize, subject to the linear dynamics $\dot{\psi}_i(t) = A_i \psi_i(t) + B_i v_i(t)$. The latter represents the linearized version of the system dynamics (3) for each mode. Variable ψ_i denotes the states of the resulting linear system, v_i consists the available control inputs at each region of operation, whereas Q_i and R_i are weight matrices. It can be shown that $v_i(t) = -K_i \psi_i(t)$ is a feedback control law that minimizes J_i with respect to the linear dynamics. The gains K_i are given by $K_i = R_i^{-1}(B_i^T P_i + Q_i^T)$, where P_i is the solution to the continuous algebraic Riccati equation $A_i^T P_i + P_i A_i + Q_i - P_i B_i R_i^{-1} B_i^T P_i = 0$.

For the gain scheduling design, and based on the analysis of Section III, v_m appears to be a natural choice for the scheduling parameter. The procedure followed can be summarized in the next steps.

- 1) Linearize the nonlinear dynamics around a family of set points that belong to the reference curves of (Fig. 4).

- 2) Compute a set of gains K_i for each linearized system by applying the LQR approach.
- 3) Interpolate the obtained sets of gains so as to achieve continuous control ([18]).

Using the same weights Q_i and R_i for all linearized systems did not result in acceptable control performance as the dynamics significantly change over the range of operating wind speeds. Therefore, setpoint dependent weights Q_i and R_i were chosen instead. Although in Region I the most significant weights are those of the speed related states, Region II includes also the power related ones. Furthermore, in both regions the off-diagonal elements in Q_i are used to penalize the additional quantities $\dot{\delta}$ and P_g . Numerical values of Q_i and R_i can be found in [22].

B. Feedback linearization

Feedback linearization provides a systematic procedure to transform a nonlinear, input affine system to a linear one, after a specific nonlinear change of coordinates and the application of a certain feedback control law. In contrast to [3], we use input-output linearization, which for the specific case appears to be a more direct approach. Further improvement over [3] is that feedback linearization is applied for both regions of operation, and hence a nonlinear controller is designed for the entire range of operating wind speeds.

Following the basic principles of feedback linearization [16], we differentiate the output until the input appears. Let $T_i(x) : \mathbb{R}^n \rightarrow \mathbb{R}^n$ be a diffeomorphic coordinate transformation, for each mode of operation i , such that

$$(3) \xrightarrow{T_i(x)} \begin{cases} \dot{\xi}_i &= A_i \xi_i + B_i [f_i^\xi(x_i) + g_i^\xi(x_i) u_i], \\ \dot{\eta}_i &= f_i^0(\xi_i, \eta_i, e), \end{cases} \quad (4)$$

where (A_i, B_i) is controllable and g_i^ξ is invertible. Variables ξ_i and η_i form the new state vector, whereas η_i represent the zero dynamics for each region. The feedback linearizing control law $u_i(t) = (g_i^\xi(x))^{-1}[v_i(t) - f_i^\xi(x)]$, renders the ξ_i dynamics linear. A feedback controller $v_i(t) = -K_i \xi_i(t)$, based on the LQR analysis of the previous subsection, can be then designed so as to achieve the desired control objectives. Since the zero dynamics η_i do not depend on the input, one should prove stability in order the feedback controller to lead in a stable closed loop system.

- 1) For Region I, $h_1(x) = \omega_r$ was chosen as output, yielding to $\xi_1 = [\omega_r \ \dot{\omega}_r]^T$ and $\eta_1 = [\delta \ w_1 \ w_2]^T$. Consequently, the original system has relative degree $\gamma = 2$. In order to achieve disturbance rejection [16], the comparably fast generator dynamics were neglected in the controller design, and T_g was treated as control input. Following (4), the dynamics of the system in the new coordinates are given by

$$\begin{aligned} \dot{\xi}_1 &= \begin{bmatrix} 0 & 1 \\ 0 & 0 \end{bmatrix} \xi_1 + \begin{bmatrix} 0 \\ 1 \end{bmatrix} (L_{\bar{f}}^2 h_1(x) + L_{\bar{C}_1} L_{\bar{f}} h_1(x) T_g), \\ \dot{\eta}_1 &= \begin{bmatrix} \dot{\delta} \\ \dot{w}_1 \\ \dot{w}_2 \end{bmatrix} = \begin{bmatrix} \omega_r - \frac{q(\omega_r, \dot{\omega}_r, \delta, w_1)}{N_g} \\ w_2 \\ -a_1 w_1 - a_2 w_2 + a_3 e \end{bmatrix}, \end{aligned}$$

where $L_{\tilde{f}}, L_{\tilde{G}_1}$ denote the Lie derivative with respect to \tilde{f} and \tilde{G}_1 , and $x = T_1^{-1}(\xi_1)$. By \tilde{f} and \tilde{G}_1 we denote the matrices resulting from (3) after neglecting the generator dynamics. The function q is a nonlinear function of $\omega_r, \dot{\omega}_r, \delta$ and w_1 . To ensure stability, the stability of the zero dynamics η should be also investigated. For this, a Lyapunov function was constructed so as to guarantee asymptotic stability of η . This is a nontrivial procedure in general, but this case exhibits a specific structure, since the nonlinearity appears only in the first state of the zero dynamics. For simplicity, the integral states $P_{g,f}, \omega_{g,f}$ were considered only in the construction of $v_i(t)$ and not in the feedback linearization procedure. Details regarding the stability of the zero dynamics can be found in [22].

- 2) For the second mode of operation $h_1(x) = \omega_g$ and $h_2(x) = P_g$ were chosen as outputs. In this case $\xi_2 = [\omega_r \dot{\omega}_r T_g]^T$ and $\eta_2 = [\omega_g \delta w_1 w_2]^T$. The resulting ξ dynamics are given by

$$\begin{aligned} \dot{\xi}_2 = & \begin{bmatrix} 0 & 1 & 0 \\ 0 & 0 & 0 \\ 0 & 0 & 0 \end{bmatrix} \xi_2 + \begin{bmatrix} 0 & 0 \\ 1 & 0 \\ 0 & 1 \end{bmatrix} \left(\begin{bmatrix} L_f^2 h_1(x) \\ L_f h_2(x) \end{bmatrix} \right) \\ & + \begin{bmatrix} L_{G_{1,u_1}} L_f h_1(x) & 0 \\ 0 & L_{G_{1,u_2}} h_2(x) \end{bmatrix} \begin{bmatrix} \theta_r \\ T_{g,r} \end{bmatrix}, \end{aligned}$$

where G_{1,u_1}, G_{1,u_2} represent the first and second column of G_1 respectively, and $x = T_2^{-1}(\xi_2)$. The vector relative degree is $\gamma = [2, 1]$. Under this choice of outputs the zero dynamics exhibit a linear behavior. To investigate their stability, set $e = 0$ and consider the error dynamics $\tilde{\eta}_2 = \eta_2 - \eta_2^*$, where $\eta_2^* = [\omega_{g,nom} \delta_{nom} 0 0]^T$ denotes the equilibrium point of the zero dynamics.

$$\dot{\tilde{\eta}}_2 = \begin{bmatrix} -\frac{D_s}{N_g^2 J_g} & \frac{K_s}{N_g J_g} & 0 & 0 \\ -\frac{1}{N_g} & 0 & 0 & 0 \\ 0 & 0 & 0 & 1 \\ 0 & 0 & -a_1 & -a_2 \end{bmatrix} \tilde{\eta}_2.$$

By inspection of the above block diagonal structure, and since all constant variables are positive, the eigenvalues will have negative real parts, and hence the zero dynamics will be asymptotically stable.

Note that for both modes of operation δ belongs to the zero dynamics, and hence cannot be directly controlled. In case fatigue reduction of the wind turbine components is the main control objective, δ should have been selected as output in the feedback linearization procedure.

C. Hybrid controller

In the previous sections turbine controllers based on gain scheduled LQR and feedback linearization were designed for each mode of operation. Hybrid controllers as part of the supervisory control [19] are necessary to ensure operation over the entire range of operating wind speeds. The switching conditions and the reset map of the hybrid model introduced

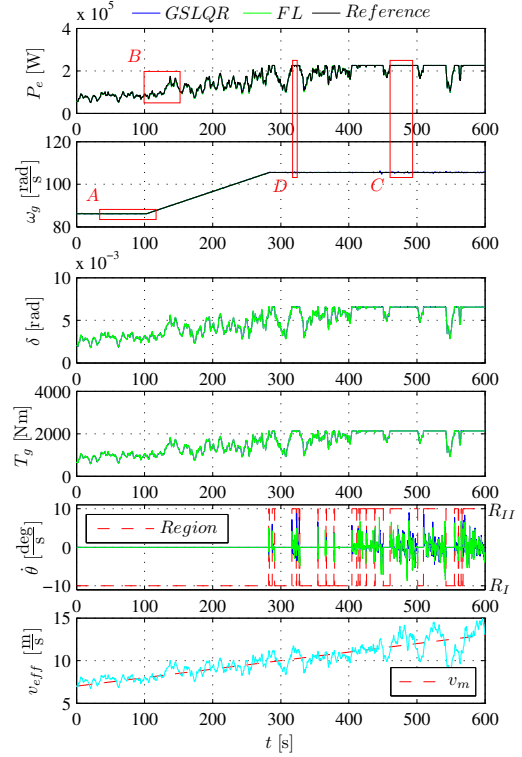


Fig. 6. Comparison between gain scheduled LQR and feedback linearization.

in Fig. 5 form the basis of the hybrid control scheme and are used both for feedback linearization and gain scheduled LQR. To further improve the performance of the hybrid controller and minimize chattering, short “hold times” of less than half a second are introduced in order to prevent the system from repeatedly changing mode. Moreover, instead of a discrete change of the gains between the two regions of operation, linear interpolation is employed.

V. SIMULATION RESULTS

Simulations have been used to investigate and compare the performance of the derived controllers. Fig. 6 shows the response of the system from low to high wind speeds. It can be seen that the references trajectories for speed and power are tracked according to the objectives defined in Section III. It should be noted that the pitch angle actuator remains within the limits ($\pm 10 \frac{\text{deg}}{\text{s}}$) over the entire simulation interval. Similarly, although no saturation is used, all states remain within their constraint set.

Fig. 7 gives insight for the case where the controllers operates in R_I mode. Both controllers stabilize the speed according to the mean wind speed (Fig. 7(a)). It is obvious that feedback linearization exhibits superior performance compared to gain scheduled LQR when considering only speed. Stabilizing the speed, however, ensures implicitly that the reference power curve is also tracked. In Fig. 7(b), the red arrow indicates that the actual power deviates from the optimum. This is always the case if v lies inside the wind interval $B - C$.

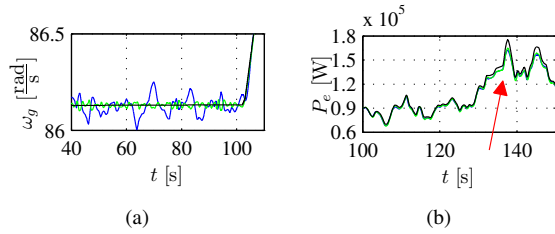


Fig. 7. Detail A (a) and B (b) of Figure 6.

Furthermore, a closer view reveals that the power curve is slightly shifted to the right when feedback linearization is used, since in that case the generator dynamics (represented by a first order transfer function), were neglected.

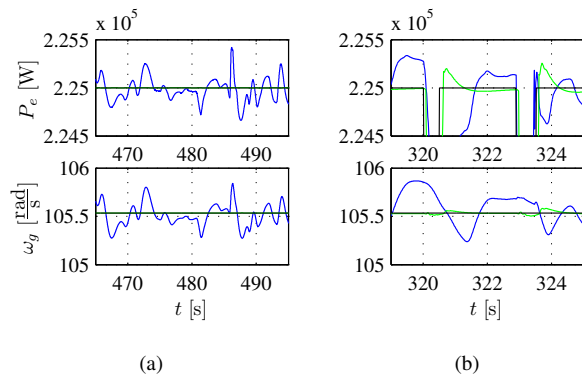


Fig. 8. Detail C (a) and D (b) of Figure 6.

The performance of the control scheme in R_{II} mode is depicted in Fig. 8(a). Although gain scheduled LQR results in some fluctuations around the reference values, feedback linearization leads to accurate tracking. Fig. 8(b) shows a detail where the two controllers change control mode several times within a few seconds. This reveals the efficiency of the proposed hybrid control scheme. It allows for fast and accurate switching between changes of the control mode, and exhibits a very good transient behavior. Chattering, which is a common issue in such applications, was alleviated, and for both controllers the overshoots were relatively low. Disturbance rejection, in the case where feedback linearization is employed, leads to perfect tracking in R_{II} , whereas in the LQR case the system fluctuates around the reference values.

VI. CONCLUDING REMARKS

In this paper a hybrid controller, based on feedback linearization, was designed for the control of a wind turbine over the entire operating region. The performance of the developed scheme was tested via simulations and was compared with standard gain scheduled LQR techniques. The feedback linearization based controller performed better in all modes of operation, and was not restricted to a local neighborhood of the operating point.

The main limitation of the proposed approach is that physical constraints on the input and state of the system are not taken into account in the control design process.

Current work concentrates on combining feedback linearization with Model Predictive Control (MPC), which allows one to solve constrained optimization problems with linear dynamics. Moreover, further investigation is needed in order to identify the robustness of the designed controllers to wind and parameter uncertainty.

VII. ACKNOWLEDGEMENT

Research was supported by the European Commission under the project MoVeS, FP7-ICT-257005, the Network of Excellence HYCON2, FP7-ICT-257462, and also KIOS Strategic project.

REFERENCES

- [1] T. Ackermann, *Wind power in power systems*. John Wiley and Sons Ltd, 2005.
- [2] M. Hansen, A. Hansen, T. Larsen, S. Øye, P. Srensen, and P. Fuglsang, "Control design for a pitch-regulated, variable speed wind turbine," Risø National Laboratory, Tech. Rep., January 2005.
- [3] S. Thomsen, "Nonlinear control of a wind turbine," Master's thesis, Technical University of Denmark, 2006.
- [4] L. Henriksen, "Model predictive control of a wind turbine," Master's thesis, Technical University of Denmark, 2007.
- [5] T. Petru, *Modeling of wind turbines for power system studies*. PhD Thesis, Chalmers University of Technology, 2003.
- [6] F. Lescher, J. Zhao, and A. Martinez, "Multiobjective h_2/h_∞ control of a pitch regulated wind turbine for mechanical load reduction," *Proceedings of the European Wind Energy Conference*, 2006.
- [7] S. Papathanassiou and M. Papadopoulos, "Mechanical stresses in fixed speed wind turbines due to network disturbances," *IEEE Transactions on Energy Conversion*, vol. 16, no. 4, pp. 361–367, 2001.
- [8] E. Bossanyi, "Wind turbine control for load reduction," *Wind Energy*, vol. 6, no. 3, pp. 229–244, July/September 2003.
- [9] E. Van der Hooft, P. Schaak, and T. Van Engelen, "Wind turbine control algorithms," ECN, Tech. Rep. ECN-C-03-111, December 2003.
- [10] B. Boukhezzer, H. Lupu, L. Siguerdidjane, and M. Hand, "Multivariable control strategy for variable speed, variable pitch wind turbines," *Renewable Energy*, vol. 32, no. 8, pp. 1273–1287, July 2007.
- [11] F. D. Bianchi, H. D. Battista, and R. J. Mantz, *Wind Turbine Control Systems*. Advances in Industrial Control, Springer Verlag, 2007.
- [12] F. Kanellos and N. Hatzigiargiou, "Control of variable speed wind turbines in islanded mode of operation," *Energy Conversion, IEEE Transactions on*, vol. 23, no. 2, pp. 535–543, jun. 2008.
- [13] M. Simoes, B. Bose, and R. Spiegel, "Design and performance evaluation of a fuzzy-logic-based variable-speed wind generation system," *Industry Applications, IEEE Transactions on*, vol. 33, no. 4, pp. 956–965, jul. 1997.
- [14] R. Rocha, L. Martins Filho, and M. Bortolus, "Optimal multivariable control for wind energy conversion system - a comparison between h_2 and h_∞ controllers," *Control and Decision Conference and European Control Conference*, pp. 7906–7911, 2005.
- [15] A. Kumar and K. Stol, "Simulating feedback linearization control of wind turbines using high-order models," *Wind Energy*, vol. 13, no. 5, pp. 419–432, July 2010.
- [16] S. Sastry, *Nonlinear Systems: Analysis, Stability, and Control*. Springer, 1999, ISBN 0-387-98513-1.
- [17] A. Isidori, *Nonlinear Control Systems*. Communications and Control Engineering Serie, Springer Verlag, 1989.
- [18] H. Khalil, *Nonlinear Systems*, 3rd ed. Prentice Hall, 2001, ISBN 978-0-19-920824-1.
- [19] K. Johnson, L. Pao, M. Balas, and L. Fingersh, "Control of variable-speed wind turbines: standard and adaptive techniques for maximizing energy capture," *Control Systems Magazine, IEEE*, vol. 26, no. 3, pp. 70–81, June 2006.
- [20] J. Højstrup, "Velocity spectra in the unstable planetary layer," *Journal of the Atmospheric Sciences*, vol. 39, no. 10, pp. 2239–2248, 1982.
- [21] J. Slootweg, H. Polinder, and W. Kling, "Dynamic modelling of a wind turbine with doubly fed induction generator," vol. 1, 2001, pp. 644–649 vol.1.
- [22] R. Burkart, *Nonlinear control of wind turbines*. Semester Project, ETH Zürich, 2010.